IOPscience iopscience.iop.org

Home Search Collections Journals About Contact us My IOPscience

Possible two-dimensional *XY* spin/gauge glasses on periodic and quasiperiodic lattices

This article has been downloaded from IOPscience. Please scroll down to see the full text article.

1997 J. Phys.: Condens. Matter 9 7141

(http://iopscience.iop.org/0953-8984/9/34/008)

View the table of contents for this issue, or go to the journal homepage for more

Download details:
IP Address: 171.66.16.209
The article was downloaded on 14/05/2010 at 10:22

Please note that terms and conditions apply.

J. Phys.: Condens. Matter **9** (1997) 7141–7159. Printed in the UK PII: S0953-8984(97)80858-2

# Possible two-dimensional *XY* spin/gauge glasses on periodic and quasiperiodic lattices

R W Reid, S K Bose and B Mitrović

Physics Department, Brock University, St Catharines, Ontario, Canada L2S 3A1

Received 10 January 1997, in final form 4 June 1997

**Abstract.** Via Monte Carlo studies of the frustrated $XY$ or classical planar model we demonstrate the possibility of a finite (nonzero) temperature spin/gauge glass-like phase in two dimensions. Examples of both periodic and quasiperiodic two-dimensional lattices, where a high-temperature paramagnetic phase appears to change to a spin/gauge glass-like phase with the lowering of temperature, are presented. The possibility of the glassy phase is supported by our study of the temperature dependence of the Edwards–Anderson order parameter, spin glass susceptibility, linear susceptibility and the specific heat. Using finite-size scaling analysis of spin glass susceptibility and the temperature dependence of the order parameter we provide estimates of critical temperatures and exponents $\eta$, $\nu$ and $\beta$ for the various lattices. On the basis of these results we expect that certain quasiperiodic as well as periodic two-dimensional arrays of superconducting grains in suitably chosen magnetic fields should behave as superconducting glasses at low temperatures.

## 1. Introduction

In a recent communication [1] we reported that the frustrated $XY$ model (see equation (1)) on a two-dimensional (2D) Penrose lattice [2] may exhibit a low-temperature spin/gauge glass phase [3, 4]. In this work, we show that quasiperiodicity is not a necessary requirement for the spin glass-like phase in this model. This conclusion is based on our Monte Carlo (MC) study of the above model on the periodic honeycomb and bathroom tile lattices. When fully frustrated, these lattices appear to undergo a transition which can be interpreted as being of paramagnetic to spin glass type. We present numerical evidence, based on our Monte Carlo (MC) simulation, that the transition temperature $T_f$ is above zero, albeit small. In addition, we find that the octagonal quasiperiodic lattice [5] exhibits a behaviour similar to that of the other three lattices, but with a somewhat higher $T_f$.

These results are unexpected in the light of the prevalent notion that the critical dimension for a spin/vortex (gauge) glass phase is greater than two [6–10]. However, a few comments and words of caution are in order at this point. As explained towards the end of the next section, our model is neither a spin glass nor a vortex or gauge glass model in the conventional sense of these terms. The element of randomness, which is essential in these models, is missing from our model. The interaction between the spins in our model is nonrandom, being determined solely by the lattice structure and an applied magnetic field. All numerical simulations [6–9] that suggest that the critical dimension for the spin glass phase is greater than two have been performed for models with random interactions between the spins. The results of these simulations thus do not apply to the present study. Schwartz and Young [10] have provided an analytical treatment showing that in dimensions $\leqslant 2$ the

0953-8984/97/347141+19$19.50 © 1997 IOP Publishing Ltd 

$XY$ spin glass order parameter should go to zero. But their proof crucially depends on configurational averaging over the (random) interactions between the spins. Such averaging is not permitted in the present case. The configurational averaging essentially makes the results independent of the lattice type, whereas the results for the frustrated $XY$ model are known to be very much lattice dependent. Thus the work of Schwartz and Young [10] does not shed any light on the behaviour of the order parameter for the frustrated $XY$ model used in this work.

In spite of the differences between our model and the conventional spin/gauge glass models the critical behaviour that we observe in our simulation is identical to that of a canonical spin glass. We have therefore decided to label the observed phase transition a spin glass transition. The frustration in the interaction between the spins, responsible for the low-temperature spin/gauge glass-like phase in this model, varies between sites in a nonrandom way determined by the lattice structure and an external field. Thus our results provide examples where frustration alone (i.e. without disorder) is capable of inducing a spin/gauge glass-like phase. Recently Lemke and Campbell [11] have studied the Ising model with nearest-neighbour random $\pm\lambda J$ and next-nearest-neighbour ferromagnetic interactions on square lattices. These authors also find evidence of a spin glass transition. It is possible that the nonrandomness of the next-nearest-neighbour interaction in their model is the key ingredient for the spin glass transition that they observe.

Our results clearly illustrate the role of lattice structure as a relevant variable from the viewpoint of the universality class of the transition. The frustrated $XY$ model has been studied widely on a variety of periodic 2D lattices using mean-field and renormalization group methods, and Monte Carlo simulation [12–25]. The results, although sometimes ambiguous and often discrepant among various authors, are certainly lattice dependent. Two most commonly reported and discussed transitions for the fully frustrated $XY$ model are the Ising type and the Kosterlitz–Thouless (KT) type [26, 27]. We provide numerical evidence that rules out the possibility of either of these two types of transition on the two periodic and the two quasiperiodic lattices considered in this work.

The purpose of this work is twofold: to provide numerical evidence that both periodic and quasiperiodic lattices should be capable of exhibiting a spin/gauge glass-like transition in 2D, and to provide some details of the study on the Penrose lattice, which were left out of our previous communication [1]. With the example of the periodic honeycomb and bathroom tile lattices we have made an attempt to dispel any misconception that we may have inadvertently generated in reference [1] that quasiperiodicity is a necessary condition for the glass-like phase in the model. Both the periodic and the quasiperiodic lattices studied in this work seem to undergo a transition which shows all the symptoms of a spin glass transition, with transition temperatures being low, but certainly above zero.

We have studied the current model without the frustration term (the $A_{ij}$-term in equation (1)), i.e. the standard $XY$ model, on the quasiperiodic 2D Penrose lattice. We find that the transition is of the KT type [26] with the exponents identical to those obtained by Tobochnik and Chester [28] in their study on the square lattice, but the transition temperature is somewhat higher. Thus in the absence of frustration (or variation in the sign of the interactions), quasiperiodicity is an irrelevant variable, as expected. The details of the standard $XY$ model study on 2D and 3D Penrose lattices will be published elsewhere.

The remainder of this paper is divided into sections as follows. In section 2 we discuss our model and some features of the lattices considered in this work. In section 3 we present the results of the MC simulations. In section 4 we compare our results with those obtained using other lattices. We also suggest what characteristic of our model might be responsible for the spin glass phase. In section 5 we present our comments and conclusions.

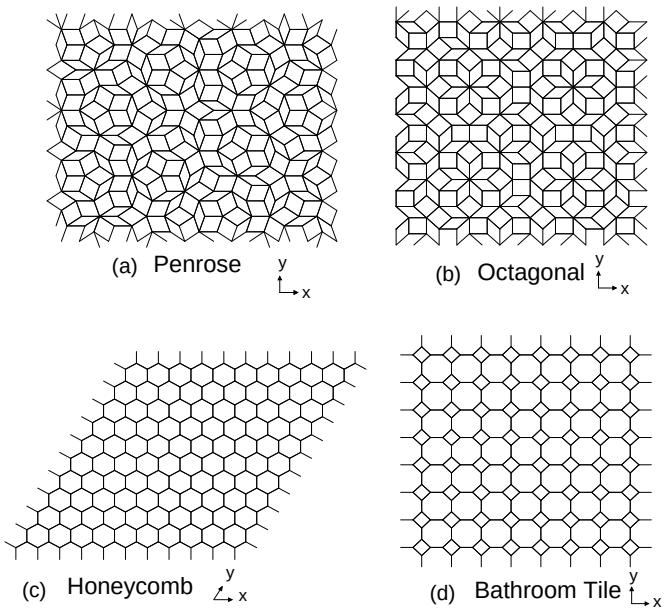


**Figure 1.** Lattices used in the present study, along with their reference frames.

## 2. The model

We consider the Hamiltonian for the $XY$ model describing the interaction between 2D spin vectors with orientations $\theta_i$ and $\theta_j$ situated at lattice sites $i$ and $j$ via a nearest-neighbour coupling parameter $J$:

$$H = -J \sum_{[ij]} \cos(\theta_i - \theta_j + A_{ij}) \tag{1}$$

where the summation is restricted to nearest-neighbour pairs $[ij]$. The parameter $A_{ij}$ controls the frustration in the model. In the context of an array of superconducting grains, $\theta_i$ is the phase of the superconducting order parameter at the grain $i$ and the above Hamiltonian can be seen as describing the resulting Josephson junction of the grains 'minimally coupled' to a transverse magnetic field with vector potential $\boldsymbol{A}$ with

$$A_{ij} = \frac{2\pi}{\Phi_0} \int_{\boldsymbol{r}_i}^{\boldsymbol{r}_j} \boldsymbol{A} \cdot \mathrm{d}\boldsymbol{l}. \tag{2}$$

$\Phi_0$ is the elementary flux quantum $hc/(2e)$ associated with the Cooper pairs, and $\boldsymbol{r}_i$ denotes the lattice sites. Here the magnetic field acts as the source of frustration: an $A_{ij}$ which is an odd multiple of $\pi$ essentially renders the bond $[ij]$ negative.

The directed sum of $A_{ij}$ about a plaquette in a 2D lattice can be written as $2\pi f$, where $f$ is the flux through the plaquette in units of $\Phi_0$. The 2D Penrose lattice [2] is composed of two (fat and thin) rhombic unit cells (plaquettes). The ratio of the areas of the fat and the thin rhombuses in the Penrose lattice is the Golden Mean ($\tau$), which is an irrational number ($(1+\sqrt{5})/2$). Thus only one set of plaquettes can be fully frustrated at a time with a suitable choice of the magnetic field giving $f = 1/2$. The flux $f$ through the individual plaquettes in the other set will then be an irrational number. The octagonal lattice [5] consists of two unit cells, one square and the other a thin rhombus, with a ratio of $\sqrt{2}$

of their areas. Similarly to the Penrose lattice case, fully frustrating one of the plaquettes results in an irrational flux through the other.

**Table 1.** The average energy per spin (site) $\langle u \rangle$ at the lowest temperature, $0.02J$, used in the simulation for various lattices and cluster sizes, $N$. $L_x$ and $L_y$ denote the linear dimensions of the clusters in the $x$- and $y$-directions, respectively.

| Lattice | $N$ | $L_x$ | $L_y$ | $\langle u \rangle$ |
|---|---|---|---|---|
| Penrose | 644 | 24.80 | 21.09 | −1.4938 |
| | 1686 | 40.12 | 34.13 | −1.4893 |
| | 4414 | 64.92 | 55.23 | −1.4889 |
| | 11 556 | 105.05 | 89.36 | −1.4884 |
| Octagonal | 239 | 14.07 | 14.07 | −1.3878 |
| | 1393 | 33.97 | 33.97 | −1.3926 |
| | 8119 | 82.01 | 82.01 | −1.3947 |
| Honeycomb | 242 | 19.05 | 19.05 | −1.2169 |
| | 1682 | 50.23 | 50.23 | −1.1980 |
| | 4050 | 77.94 | 77.94 | −1.1926 |
| | 8192 | 110.85 | 110.85 | −1.1868 |
| Bathroom tile | 256 | 19.31 | 19.31 | −1.1842 |
| | 1600 | 48.28 | 48.28 | −1.1846 |
| | 4096 | 77.25 | 77.25 | −1.1843 |
| | 8100 | 108.64 | 108.64 | −1.1847 |

Figure 1 displays the lattices used in this work along with the reference $x$- and $y$-directions. The linear dimensions of the clusters used in the simulation along the $x$- and $y$-directions, $L_x$ and $L_y$, and the corresponding numbers of sites in the clusters are given in table 1.

In figures 1(a) and 1(b) we show sections of Penrose (decagonal) and octagonal quasilattices. Self-similarity, or, equivalently, the inflation–deflation property of these two quasilattices, is characterized by two irrational numbers, the Golden Mean ($\tau = (1 + \sqrt{5})/2$) and the Silver Mean ($\sigma = 1 + \sqrt{2}$), respectively, which also dictate their decagonal and octagonal bond orientational symmetry. The two quasilattices can be generated via projections of 5D and 4D simple hypercubic (periodic) lattices onto the physical 2D plane. They have similar ring structure, both containing only even-order rings. The average number of nearest neighbours for both quasilattices is four, as in a square lattice. But unlike the square lattice, the two quasilattices are characterized by variations in near-neighbour environments. For the Penrose (decagonal) lattice the number of nearest neighbours varies between three and seven, whereas for the octagonal lattice the number varies between three and eight. In order to reduce the surface effects in our finite-cluster MC calculations we have used periodic boundary conditions. Rational approximants of the two quasilattices, which can be repeated periodically, can be obtained from the rational approximations of the irrational numbers, the Golden and the Silver Means. We follow a systematic way to generate these periodic approximants as given by Lançon and Billard [29].

Figures 1(c) and 1(d) display sections of the two periodic lattices, honeycomb and bathroom tile, considered in the present work. Note that both are non-Bravais lattices with the same number of nearest neighbours. The smallest unit cells that provide a Bravais lattice description of these lattices involve two sites for the honeycomb lattice and four for the bathroom tile. The honeycomb lattice consists of only one type of plaquette (hexagonal),

while the bathroom tile lattice has two types, square and octagonal, with an irrational ratio of $4(1+\sqrt{2})$ of the areas of the two plaquettes (octagonal to square). Both structures contain only even-order rings.

Finally, a word about the nomenclature used to describe the model given by equation (1). If the $A_{ij}$ are restricted to the values 0 and $\pi$ and randomly assume these values with equal probability, then the model becomes the Edwards–Anderson $\pm J$ $XY$ spin glass, with random ferromagnetic ($A_{ij}=0$) or antiferromagnetic ($A_{ij}=\pi$) coupling between adjacent spins. If the $A_{ij}$ are independent random variables, assuming all values between 0 and $2\pi$, the model is referred to as the gauge or vortex glass model [30] and is believed to belong to a different universality class, presumably because it lacks the 'reflection' symmetry, $\theta_i \rightarrow -\theta_i$ $\forall i$. In the present case the $A_{ij}$ are lattice structure dependent. They assume many different values in the interval between 0 and $2\pi$, determined strictly by the lattice structure and the applied transverse field. In this sense our model is different from both the spin glass and gauge glass models. However, we will use the term spin glass throughout the remainder of this paper, especially in describing the phase transition itself. The quantities that we study show temperature variations similar to those observed experimentally for the so-called spin glasses, hence the choice.

## 3. Results of MC simulation

For the lattices which contain two different plaquettes, we present results for the case where the plaquettes with the smaller area are fully frustrated. For the Penrose lattice these are the thin rhombohedral plaquettes. For the octagonal and the bathroom tile lattices these are, respectively, the rhombohedral and the square plaquettes. Results for the other case, where the plaquettes with the larger area are fully frustrated, are qualitatively similar. All of our results are obtained via MC simulation based on the Metropolis algorithm [31], using periodic boundary conditions. We have cooled our systems in a quasistatic manner, starting from a high-temperature ($T$(in units of $J$) $> 2.0$) random configuration and then heated the system in the same quasistatic fashion. Since we performed the simulation in $n$ blocks, the heating and cooling data are obtained by averaging over these blocks, with the error bars representing the standard deviation, obtained by dividing the square root of the sum of squares of the deviations from the mean by $\sqrt{n-1}$, instead of $\sqrt{n}$. We then perform a 'grand average' over the heating and cooling data.

By associating a spin $\boldsymbol{S}_i = (\cos\theta_i, \sin\theta_i)$ with every lattice site $i$, we can define the quantity

$$\frac{1}{N}\sum_{i}^{N}\langle \boldsymbol{S}_i \rangle \tag{3}$$

where $\langle\ \rangle$ denotes a canonical ensemble average at a temperature $T$, as the magnetic moment per site at temperature $T$. Note that this quantity does not represent the actual magnetic moment of a cluster of superconducting grains in a transverse magnetic field. However, defined as above, the magnetic moment per lattice site calculated for all of the lattices studied is found to be small ($<0.02$) over the entire temperature range. The magnitude of the moment decreases steadily with the size of the cluster, suggesting that the magnetization is strictly zero in the thermodynamic limit. For the largest lattice studied ($N = 11\,556$) the magnetic moment per lattice site is $<0.006$, i.e. zero for all practical purposes. For all lattices and lattice sizes the magnetic moment shows no discernible temperature dependence, staying practically zero at all temperatures. This is an indication that the ground state (more

appropriately, the lowest-temperature ($0.02J$) state studied via our MC simulation) retains the continuous O(2) symmetry of the Hamiltonian, and there is no spontaneous breakdown into the discrete Z(2) symmetry, as would be the case for an Ising transition. However, the vanishing of the magnetic moment at all temperatures does not rule out the possibility of a KT transition. Below we present further analysis in an attempt to determine the existence and nature of the transition(s) for the various lattices.

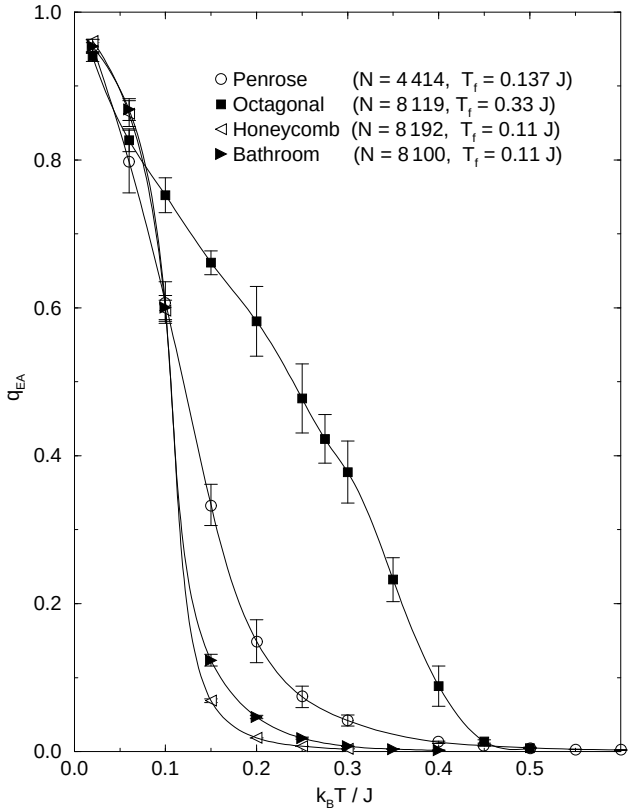


**Figure 2.** The Edwards–Anderson order parameter as a function of temperature. $N$ denotes the number of lattice sites and $T_f$ is the estimate of the transition temperature for the corresponding lattice, obtained from the analysis of the spin glass susceptibility.

### *3.1. The Edwards–Anderson order parameter*

Since the spins appear to be disordered at all temperatures, it is appropriate to explore the possibility of spin freezing over macroscopic timescales. To study the freezing of the spins at the lattice sites we calculate the Edwards–Anderson [32] order parameter. In figure 2 we show this order parameter, defined by

$$q_{EA} = (1/N)\sum_{i}^{N}\langle \boldsymbol{S}_i\rangle^2. \tag{4}$$

In a completely frozen system $q_{EA}$ is unity, while for a completely ergodic system it is zero. This order parameter shows a monotonic decrease with increasing temperature, clearly

vanishing at temperatures beyond 0.5 for all lattices. The results shown in figure 2 were obtained by averaging over 5 blocks of 60 000 configurations, generated after equilibrium was achieved. In all cases the order parameter is seen to vanish not abruptly, but continuously with a long tail. This is a consequence of the finite system size. It is expected that the tail region will decrease with increasing system size and eventually disappear in the thermodynamic limit. We find that the tail persists, even for our largest systems (e.g. ∼11 000-site cluster for the Penrose lattice) and, consequently, the transition temperature, at which $q_{EA}$ goes to zero, cannot be appropriately determined from figure 2. Thus, we use other quantities to analyse the transition and provide estimates of the transition temperatures $T_f$ for the four lattices. In figure 2, we have indicated, in addition to the lattice sizes, our estimates of the transition temperatures for the corresponding lattice, obtained from a finite-size scaling analysis of spin glass susceptibility (to be described later).

Although we cannot accurately determine a $T_f$ from this method, it is clear that all of the systems studied have a low-temperature spin/gauge phase with a nonzero order parameter $q_{EA}$, changing into a phase with zero $q_{EA}$ as the temperature is raised.

### *3.2. Linear susceptibility*

Linear susceptibilities per spin for the honeycomb lattice, calculated from the fluctuations in the magnetization (net magnetic moment $|m|$ for a lattice of $N$ sites),

$$\chi = \frac{\langle m^2 \rangle - \langle |m| \rangle^2}{N k_B T} \tag{5}$$

are shown in figure 3. At low temperatures (0.02–0.2)$J$, the results are obtained by averaging over 5 blocks of 125 000 MC steps, while 5 blocks of 15 000–45 000 steps were used for higher temperatures. The large hysteresis in the low-temperature region indicates a high number of metastable states, which is a characteristic of spin glasses. These metastable states give rise to large error bars in $\langle m^2 \rangle - \langle |m| \rangle^2$ at low temperatures, which are further accentuated by a division by $T$ in equation (4). Although we feel that it might be possible to reduce the size of these error bars, this would require very long runs and one must also ensure that the system does not become trapped in one of these metastable states. Nevertheless, despite the large error bars, a cusp-like feature in $\chi$ is clearly visible around $T_f \sim 0.15$. We also find a saturation in this cusp with respect to system size, which is consistent with spin glass behaviour. The behaviour of the susceptibility for the honeycomb lattice shown in figure 3 is very similar to that for the Penrose lattice, discussed in our earlier publication [1].

In the inset of figure 3 we have shown the quantity $T\chi$, which approaches a constant at high-temperatures. Thus the high-temperature phase is strictly paramagnetic with $\chi$ obeying the Curie law. The general temperature dependence of $T\chi$ for all other lattices studied, Penrose, octagonal and bathroom tile, is similar to that shown in figure 3. The Penrose lattice result is given in reference [1]. Note that since the magnetic moment $\langle m \rangle \sim 0$ for all the lattices, the quantity plotted in the inset of figure 3 is proportional to $\langle m^2 \rangle$. For a KT transition this quantity diverges below the transition temperature. For an Ising-type (paramagnetic-to-ferromagnetic) transition it remains finite as the temperature approaches zero, and also is dependent on the system size. Thus the fact that $\langle m^2 \rangle$ approaches zero for all of the lattices studied is an indication that they do not exhibit either KT or Ising-type transition as the temperature is lowered from the high-temperature paramagnetic phase. The saturation of the susceptibility with the system size, the appearance of a cusp-like feature and the vanishing of the function $\langle m^2 \rangle$ as the temperature approaches zero are all consistent

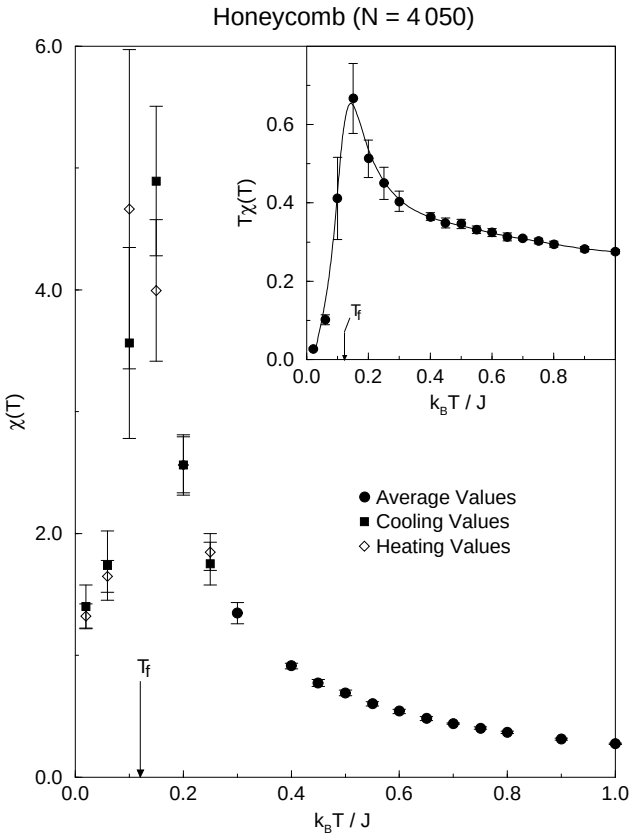


**Figure 3.** The linear susceptibility as a function of temperature for the honeycomb lattice. The inset shows the product $T\chi$, clearly indicating that the high-temperature phase is paramagnetic, with a Curie-like behaviour for $\chi$.

with the scenario of a low-temperature spin glass phase. As mentioned earlier, the variation of $\langle m^2 \rangle$ or $T\chi$ with temperature for the other lattices is similar to that shown in the inset of figure 3, although some irregular features seem to appear in the function $\chi$ itself for the octagonal and the bathroom tile lattices, as the division by $T$, especially at low temperatures, strongly magnifies minor deviations in $\langle m^2 \rangle$ from their exact values. For all four lattices studied $\langle m^2 \rangle$ rises, more or less smoothly, from zero and saturates at a constant value as the temperature is increased. Note that the bump in the inset of figure 3 is probably due to a convergence problem, as indicated by the large error bars. The results for the Penrose lattice do not show such a bump (see the inset of figure 2 in reference [1]).

It should also be noted that we have repeated the susceptibility calculation for the Penrose lattice without the frustration term $A_{ij}$ in equation (1). We obtain a divergence in susceptibility as the temperature is lowered, consistent with a KT transition. By fitting the susceptibility to the form proposed by Kosterlitz [27] we have obtained a KT transition temperature $T_{KT}$ of $1.027 \pm 0.002J$ for this lattice and an exponent in agreement with that obtained by Tobochnik and Chester [28] for the square lattice. The value of 1.027 for $T_{KT}$ obtained by us for the Penrose lattice is slightly higher than the value (0.89–0.95)$J$ reported in the literature for the square lattice (see Tobochnik and Chester [28] and references therein). Details of the unfrustrated Penrose lattice calculation will be published elsewhere.

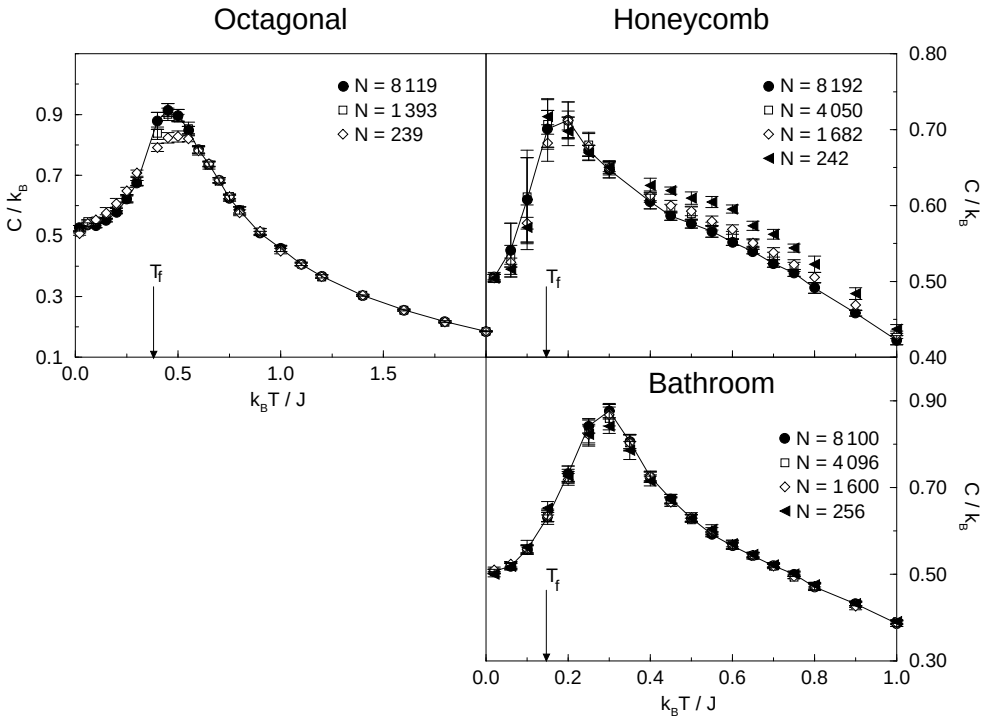


**Figure 4.** The specific heat as a function of temperature for the octagonal, honeycomb and bathroom tile lattices.

### *3.3. Specific heat*

The temperature variation of the specific heat for both frustrated and unfrustrated Penrose lattices has been discussed in our earlier publication [1]. The specific heat per site for the two periodic lattices and the octagonal lattice obtained from the fluctuations in the energy $U$ of the system:

$$C = \frac{\langle U^2 \rangle - \langle U \rangle^2}{N k_B T^2} \tag{6}$$

are shown in figure 4. The results for various system sizes, clearly indicating a saturation with respect to system size, are shown. These results are averages between heating and cooling, with the low-temperature results having a somewhat larger hysteresis. All of the averages were obtained after equilibrating; however, the high-temperature values were obtained by averaging over 5 blocks of 15 000 steps, whereas 5 blocks of 45 000 steps were used for the low temperatures. The saturation in the peak height of the specific heat is a consequence of the fact that it appears at a temperature at which the spin glass correlation is finite, i.e. above the spin/gauge glass transition temperature. Note that for all lattices the zero-temperature specific heat approaches a value of $0.5k_B$. This is consistent with the equipartition theorem valid for the Hamiltonian (1) with the cosine function being truncated at the quadratic term.

A few comments regarding our results on the honeycomb lattice are in order at this stage. Shih and Stroud [13] carried out a Monte Carlo study of the fully frustrated $XY$

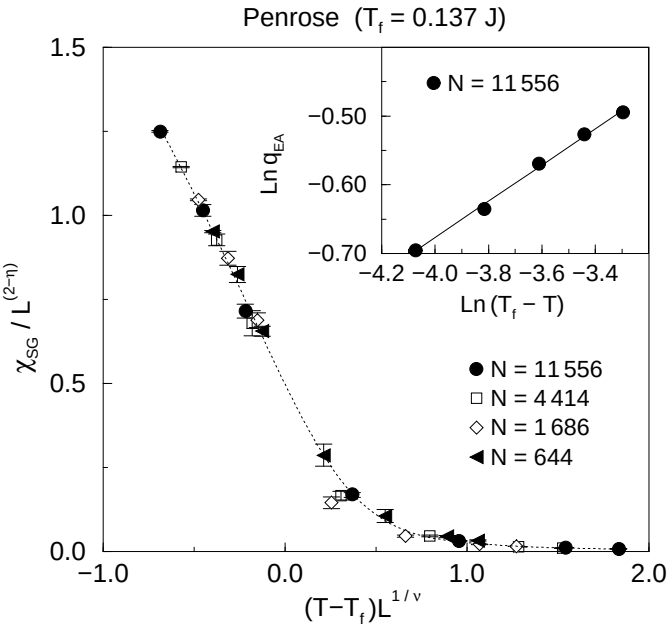


**Figure 5.** A scaling plot of the spin glass susceptibility for the Penrose lattice obtained using the exponents $\eta = 0.2$, $\nu = 2.6$, and $T_f = 0.137$. The inset shows the log–log plot of the Edwards–Anderson order parameter versus $T_f - T$ with $T_f = 0.137$. The slope of this plot yields a value of 0.26 for the exponent $\beta$, in perfect agreement with the hyperscaling relation $\beta = \nu\eta/2$. See the text and table 2 for details.

model on the honeycomb lattice and reported the nature of the transition as KT. Their study on the honeycomb lattice was carried out together with a study of the triangular lattice, and the conclusions regarding the nature of the transition, Ising versus KT, were primarily based on the saturation of the specific heat with respect to system size. For the honeycomb lattice a saturation in the specific heat was obtained, while the triangular lattice did not show any saturation. Consequently, the transitions were classified as KT and Ising-type for the fully frustrated $XY$ model on honeycomb and triangular lattices, respectively. Our work on the honeycomb lattice shows that the conclusion drawn by Shih and Stroud [13] was premature, since the susceptibility for the honeycomb lattice shows no divergence characteristic of a KT transition. Our results for the specific heat agree numerically with the results of Shih and Stroud. In addition our results for the system energy at the lowest temperature studied ($0.02J$) agree with the ground-state energy reported by Shih and Stroud [13]. In table 1 we present the average energy per spin for all of the lattices and cluster sizes used in the simulation. We find that with periodic boundary conditions magnetic moments or ferromagnetic correlations decrease with increasing system size at low temperatures, yielding higher energy per spin for larger sizes. For the 256-site honeycomb lattice our value of the average energy per site at $T = 0.02J$, $-1.2169J$, is lower than the ground-state energy of $-1.2071J$ reported by Shih and Stroud [13]. Presumably, Shih and Stroud report the value obtained for their largest cluster of 576 sites. For a 1600-site cluster our value of the energy at $0.02J$, $-1.198J$, is slightly higher. In addition to specific heat and energy, our results for $q_{EA}$ are in good agreement with the local order parameter values reported by Shih and Stroud [13]. Note that the local order parameter studied by Shih and

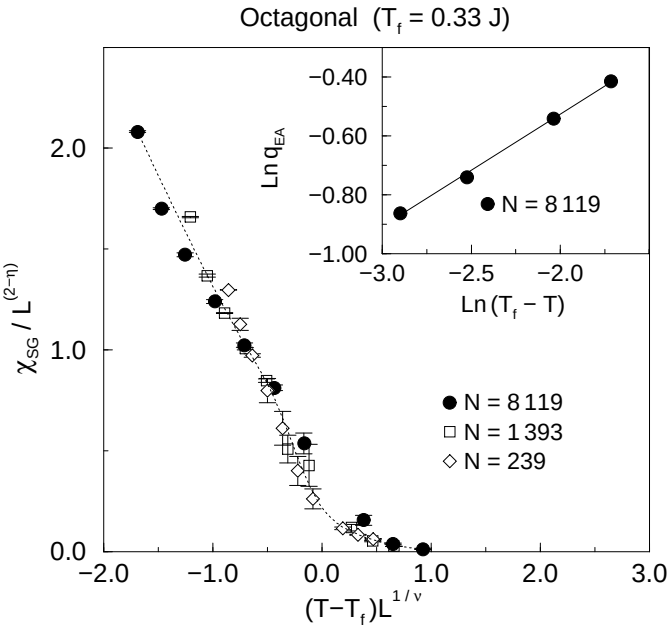


**Figure 6.** A scaling plot of the spin glass susceptibility for the octagonal lattice obtained using the exponents $\eta = 0.3$, $\nu = 2.6$, and $T_f = 0.33$. The slope of the log–log plot in the inset is 0.38, in agreement with the hyperscaling relation $\beta = \nu\eta/2$. See the text and table 2 for details.

Stroud is the square root of the order parameter $q_{EA}$ studied in this work. On the basis of these comparisons it appears that the study by Shih and Stroud was correct in terms of the accuracy of the quantities reported, but incomplete as regards correctly identifying the nature of the transition.

### *3.4. Spin glass susceptibility*

In a ferromagnet, the approach to the ferromagnetic phase from temperatures above the Curie temperature $T_C$ is accompanied by a dramatic increase in the range of the spin correlations, which then diverges at $T_C$. A corresponding phenomenon occurs in spin glasses. However, it is not the spin correlation function $\langle \boldsymbol{S}_i \cdot \boldsymbol{S}_j \rangle$, but rather its square that acquires a long range. This leads to the divergence, at the spin glass transition temperature $T_f$, of the spin glass susceptibility

$$\chi_{SG} = \frac{1}{N} \sum_{ij} \langle \boldsymbol{S}_i \cdot \boldsymbol{S}_j \rangle^2 \qquad (T > T_f). \tag{7}$$

$\chi_{SG}$ satisfies a finite-size scaling relation of the form [6]

$$\chi_{SG} = L^{2-\eta} \bar{\chi}(L^{1/\nu}(T - T_f)) \tag{8}$$

where $\bar{\chi}$ is the scaling function, $L$ is the system length, $\nu$ is the exponent for the spin glass correlation length $\xi$ for $T \geqslant T_f$, and $\eta$ describes the power-law decay of the spin glass correlation at $T_f$. For the quasiperiodic lattices the linear dimensions in the $x$- and $y$-directions, $L_x$ and $L_y$, are different. Thus the scaling relations could be studied using either of these two as a measure of the linear dimension of the cluster. Alternatively, one

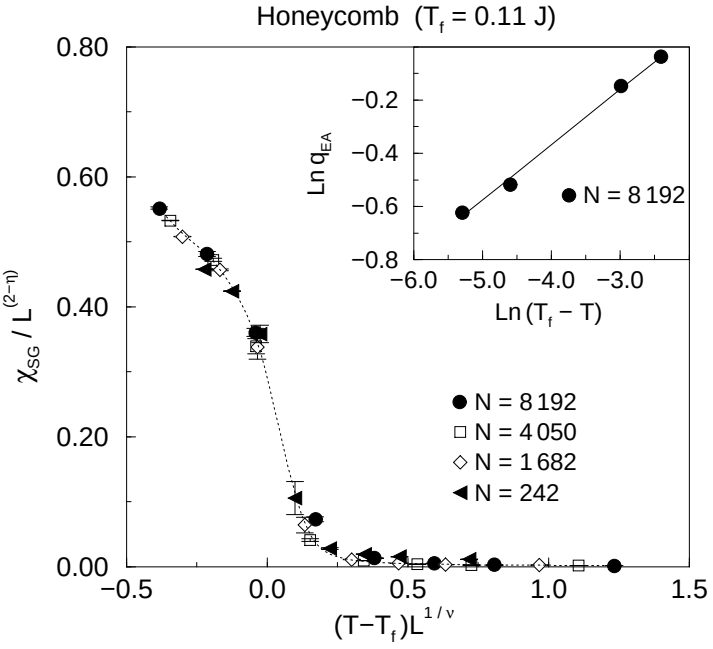


**Figure 7.** A scaling plot of the spin glass susceptibility for the honeycomb lattice obtained using the exponents $\eta = 0.12$, $\nu = 3.25$, and $T_f = 0.11$. The slope of the log–log plot in the inset is 0.207, in good agreement with the hyperscaling value 0.195. See the text and table 2 for details.

could use $L = \sqrt{N}$ as a measure of the linear dimension of a cluster of $N$ sites. All three options give similar results for all of the lattices that we have studied. In the following, we will present results with $L_x = L$ in equation (7). To ensure a proper convergence of $\chi_{SG}$, calculated via equation (6), we have averaged over 5 blocks of 40 000–60 000 steps at low temperatures ($<0.2J$) and 5 blocks of 60 000–80 000 steps at higher temperatures. By examining our results every 5000 steps, we find, for all lattices, little change in $\chi_{SG}$ over the last 5000–10 000 steps. Thus, we estimate that these chain lengths produce at least a 95% convergence in $\chi_{SG}$.

**Table 2.** The spin glass transition temperature $T_f$ and the exponents $\eta$ and $\nu$ obtained for the various lattices from finite-size scaling analysis of the spin glass susceptibility. The exponent $\beta$ is obtained from the log–log plot of the Edwards–Anderson order parameter $q_{EA}$ and $T - T_f$. According to the hyperscaling relation the exponent $\beta$ should equal $\nu\eta/2$, which is shown in column 4. The error estimates result from attempting to fit the scaling relation, equation (8), together with the hyperscaling relation $\beta = \eta\nu/2$ (see the discussion in the text). The error bars for $T_f$ are within 10%.

| Lattice | $T_f$ | $\eta$ | $\nu$ | $\beta$ | $\nu\eta/2$ |
|---|---|---|---|---|---|
| Penrose | 0.137 | $0.20 \pm 0.03$ | $2.6 \pm 0.4$ | $0.263 \pm 0.009$ | 0.26 |
| Octagonal | 0.33 | $0.30 \pm 0.02$ | $2.6 \pm 0.4$ | $0.38 \pm 0.01$ | 0.39 |
| Honeycomb | 0.11 | $0.12 \pm 0.02$ | $3.25 \pm 0.6$ | $0.207 \pm 0.009$ | 0.195 |
| Bathroom tile | 0.11 | $0.12 \pm 0.02$ | $3.25 \pm 0.6$ | $0.214 \pm 0.007$ | 0.195 |

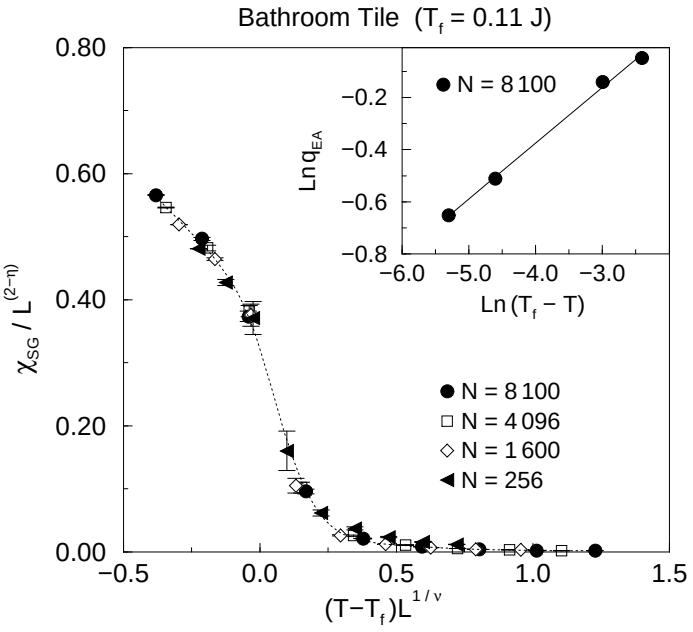


**Figure 8.** A scaling plot of the spin glass susceptibility for the bathroom tile lattice obtained using the exponents $\eta = 0.12$, $\nu = 3.25$, and $T_f = 0.11$. The slope of the log–log plot in the inset is 0.214, in good agreement with the hyperscaling value 0.195. See the text and table 2 for details.

In figures 5–8 we show the scaling behaviour of $\chi_{SG}$ in terms of $L_x$. In table 2 we provide our estimates of the critical exponents $\nu$, $\eta$ and $\beta$ and the critical temperatures $T_f$ for the various lattices. The best way to obtain the critical temperature is via the fourth-order cumulant (Binder parameter) of the order parameter [33]. Bhatt and Young [6], in their study of the $\pm J$ Ising spin glasses, calculated the cumulant from the probability distribution of the order parameter $q$. This method of obtaining the cumulant is inapplicable in the present case, where the effective bond interactions are not random variables. The cumulant could be obtained from a direct calculation of the multi-spin correlation functions for the various lattices, with preassigned flux through the plaquettes. However, stringent requirements of both computer memory and time render such calculations beyond our present available resources. Thus we have combined the finite-size scaling equation (7) with the hyperscaling relation $\beta = \eta\nu/2$ to obtain reliable estimates of $T_f$ and the exponents. We find that small changes in $T_f$ in equation (7) can lead to significant changes in the exponents $\eta$ and $\nu$, if the latter are allowed unrestricted variations. However, the constraint $\beta = \eta\nu/2$ and equation (7) can be simultaneously satisfied only if $T_f$ is pinpointed accurately. In the insets of figures 5–8 we show the log–log plots of the Edwards–Anderson order parameter versus $T - T_f$. The exponents $\beta$, obtained from these log–log plots, are then required to satisfy the hyperscaling relation for $\eta$ and $\nu$ obtained from equation (7). The error bars for $\eta$ and $\nu$ provided in table 2 are estimates resulting from good fits to equation (7), once $\beta$ and $T_f$ are known fairly well from the $\log(q_{EA})$ versus $\log(T_f - T)$ plots. The error bars for $T_f$ are less than 10%.

In figure 9 we show a fit to the finite-size scaling equation (7) for the Penrose lattice with $T_f$ set equal to zero. Note that this results in an unusually high value of $\nu$ and a very

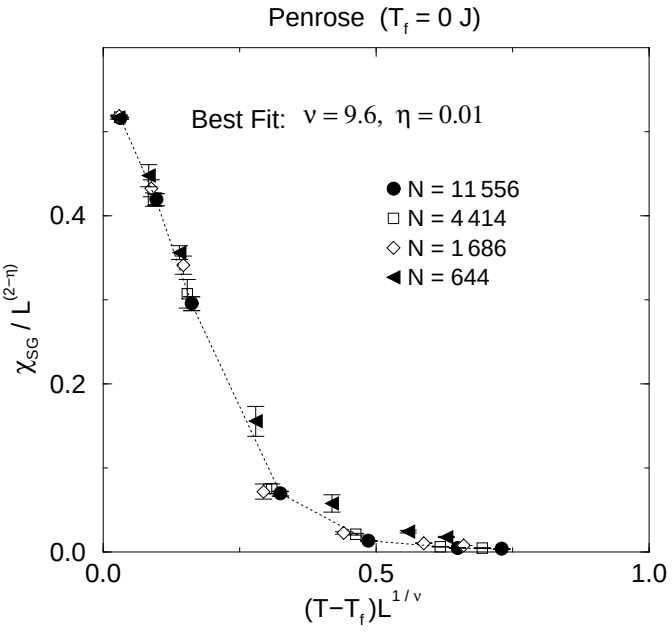


**Figure 9.** A scaling plot of the spin glass susceptibility for the Penrose lattice with $T_f = 0$. See the text for details.

small value of $\eta$. The near-zero (0.01) value of $\eta$ implies that the correlation function $\Gamma(\boldsymbol{r})$ of the square of the quantity $\langle \boldsymbol{S}_i(0) \cdot \boldsymbol{S}_j(\boldsymbol{r}) \rangle$ becomes almost independent of $\boldsymbol{r}$ at $T_f$:

$$\Gamma(\boldsymbol{r}) \sim \frac{1}{\boldsymbol{r}^{d-2+\eta}} \tag{9}$$

at $T = T_f$ in dimension $d$. This, in turn, means that the spins are either parallel or antiparallel at $T_f$, a highly unlikely scenario in view of the frustration varying from site to site and giving rise to a large number of effective bond interactions (see figure 10). No evidence of such spin alignments is found in snapshots taken from our simulation at the lowest temperature (0.02). Note, in addition, that a zero freezing temperature would be clearly inconsistent with our results for the Edwards–Anderson order parameter and linear susceptibility. Since an equally good fit, consistent with all of our results and satisfying equation (7) as well as the hyperscaling relation $\beta = \eta\nu/2$, can be obtained for $T_f \neq 0$, we decide in favour of the latter scenario. The same comment applies to all other lattices examined in this work.

We note that the exponents for the various lattices are very similar (those for the two periodic lattices being identical). In principle, in the presence of lattice-structure- and site-dependent nonrandom frustration, each lattice type can belong to a different universality class. It is interesting to note, however, that the exponents obtained in this work for the frustrated $XY$ model are similar to those obtained by Bhatt and Young [6] in their study of the $\pm J$ Ising model in 2D (square lattice) ($T_f = 0$): $\eta = 0.2 \pm 0.05$, $\nu = 2.6 \pm 0.4$. In particular, for the Penrose lattice the agreement with the exponents for the $\pm J$ Ising model is remarkable. However, since $T_f$ is found to be zero for the latter case [6], the universality class for the frustrated $XY$ model on a Penrose lattice ($T_f \neq 0$) is deemed to be different, according to the present work, from that of the $\pm J$ Ising spin glass in 2D. The equality of

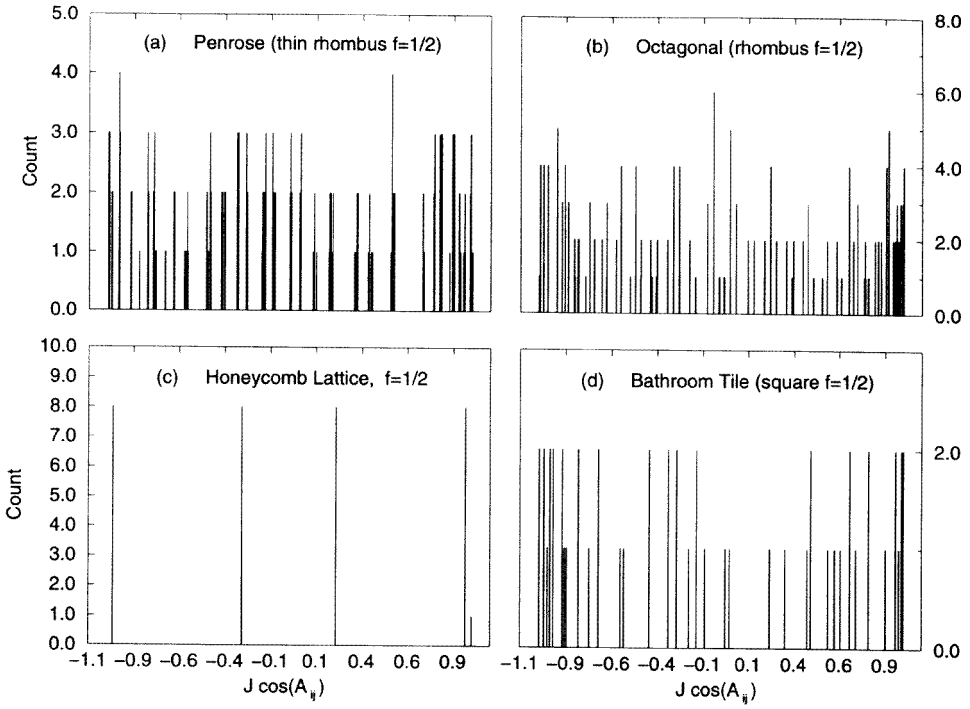


**Figure 10.** The distribution of the effective nearest-neighbour coupling parameter $\cos(A_{ij})$ for the lattices used in this work.

the exponents in the two models is most probably fortuitous, but is certainly interesting and worth exploring. For comparison, the exponents for the $\pm J$ $XY$ model in 2D (with $T_f = 0$), obtained by Jain and Young [7], are: $\eta = 0.3 \pm 0.3$, $\nu = 1.08 \pm 0.27$. We emphasize that the model that we have studied is, strictly speaking, neither a spin glass nor a vortex glass model (as explained in section 2), and invokes a frustration that is dependent on the lattice structure. Each lattice in this model can belong to a different universality class, which should in turn be different from the universality classes corresponding to the spin glass and vortex glass models in 2D. An interesting observation is that the exponents for the two periodic lattices and the corresponding $T_f$ are almost identical, and the exponents for the two quasiperiodic lattices are very close. The differences in the values of the exponents are certainly larger between a quasiperiodic and a periodic lattice than between two periodic or quasiperiodic lattices. Also, quasiperiodic lattices appear to have a higher $T_f$ than the periodic ones. Because we have examined only two periodic and two quasiperiodic lattices, the speculative nature of these statements cannot be overlooked.

## 4. Comparison with results on other lattices

As stated in the introduction, the frustrated $XY$ model has been studied on a variety of 2D lattices, the most widely studied being the square and the triangular ones. Although there is some controversy regarding the nature of the transition on these lattices, including the issue of the existence of more than one transition, most authors report the nature of the transition on these two lattices as being 'Ising-like'. It will be useful to identify some feature of the

model on the lattices studied in the present work that distinguishes these from the square or triangular lattice. The obvious quantity to look at is the distribution of the lattice-dependent vector potentials $A_{ij}$. Equivalently, we could rewrite equation (1) as

$$H = \sum_{[ij]} -J\cos(A_{ij})\cos(\theta_i - \theta_j) + \sum_{[ij]} J\sin(A_{ij})\sin(\theta_i - \theta_j) \tag{10}$$

where the first term is simply the standard $XY$ Hamiltonian, with the lattice-dependent frustration appearing via the variation in the effective nearest-neighbour exchange parameters $\cos(A_{ij})$. We thus look at the distribution of the effective coupling parameters, or simply the quantity $\cos(A_{ij})$ for various lattices.

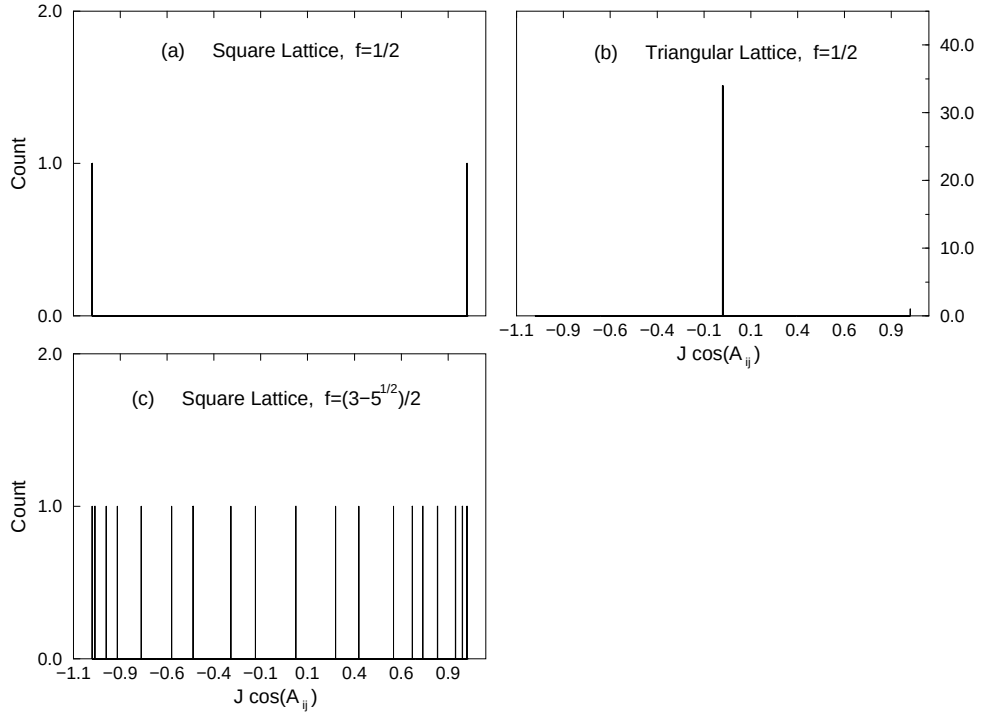


**Figure 11.** The distribution of the effective nearest-neighbour coupling parameter $\cos(A_{ij})$ for the fully frustrated triangular and square lattices, and for square lattice with an irrational flux, $f = (3 - \sqrt{5})/2$, through the plaquettes.

In figure 10 we show this quantity for the lattices studied in this work and in figure 11 we show the same for the fully frustrated square and the triangular lattices. The square and the triangular lattices, which show the Ising-like transition, have far fewer values of the parameter $\cos(A_{ij})$ than all of the other lattices exhibiting spin glass behaviour. It should be noted that in order to compare the distribution of the quantity $\cos(A_{ij})$ for various lattices, we chose, in each case, the reference $x$- and $y$-axes along some symmetry direction of the lattice. An arbitrary choice of the reference axes, without any regard to the symmetry of the lattice, may result in a distribution showing spuriously large values of the parameter $\cos(A_{ij})$. Such values of $\cos(A_{ij})$ give rise to frustration which can be simply gauged away by rotating the reference frame used to describe the lattice sites, and cannot be responsible

for spin glass behaviour [4, 34]. In figure 11 we also show the distribution of $\cos(A_{ij})$ for a square lattice with an irrational flux, $f = (3-\sqrt{5})/2$, through the plaquettes. This model was studied by Halsey [35], and was reported to show a low-temperature spin glass phase. We note that the distribution of $\cos(A_{ij})$ for this case is similar to the distribution for the four cases studied by us, showing a large number of possible values.

From the above discussion it appears that frustrated $XY$ models with a wide and more or less uniform distribution of the effective coupling parameters (more appropriately with a large number of values of the parameter $\cos(A_{ij})$ distributed over the interval between $-1$ and 1) belong to a different universality class to those with only a few possible values of $\cos(A_{ij})$. It is conceivable that for the square and the triangular lattices, with only two to three possible values of the effective coupling constant, the low-temperature phase is a spin-ordered state with a nonzero wave vector. This leads to a normal second-order phase transition with the specific heat showing a lack of saturation with respect to the system size and diverging at the transition temperature, as observed by Teitel and Jayaprakash [12] and Shih and Stroud [13]. An increase in the number of possible values of the effective coupling parameter leads to a scenario where the spin disorder persists at all temperatures. This is the case for all of the lattices, periodic and quasiperiodic, studied in this work. Our detailed numerical study shows that the low-temperature phase for these lattices differs from the high-temperature phase in that the spins at low temperatures are frozen over macroscopic timescales, while at high temperatures they are free. The numerical evidence that there must be an order-of-magnitude change in timescales over which the spins rotate is strong. That the lattice structure is a relevant variable for the frustrated $XY$ model has been known for a long time. Here we point out a feature dependent on both the lattice structure and the magnetic field, namely the distribution of the parameter $\cos(A_{ij})$, that might account for the spin/gauge glass-like phase in the model.

We would like to remind the reader that the parameter $\cos(A_{ij})$ in the above discussion is nonrandom. The above discussion is strictly limited to the frustrated $XY$ model, and does not apply to conventional gauge/spin glass models with random interaction between the spins.

## 5. Comments and conclusions

In summary, we have presented numerical evidence in support of the existence of a low-temperature spin/gauge glass phase for the frustrated $XY$ model on two quasiperiodic (Penrose and octagonal) and two periodic (honeycomb and bathroom tile) lattices. Our interpretation of the nature of the transition or the low-temperature phase is based on the temperature dependence of the Edwards–Anderson order parameter, spin glass susceptibility, linear susceptibility, and the specific heat, obtained via Monte Carlo simulation. While we cannot absolutely rule out an alternative explanation of our results, the numerical evidence in support of our interpretation is strong. The magnetization is found to be zero (as close to zero as possible in any numerical simulation) at all temperatures for all of the lattices studied. We have also carried out a detailed study of the unfrustrated ferromagnetic $XY$ model on the Penrose lattice. The results are similar to those for a square lattice [28], with a slightly higher KT transition temperature.

Of all of the lattices studied in this work, only the honeycomb lattice has been studied previously in connection with the frustrated $XY$ model, by Shih and Stroud [13]. Our results for the order parameter, specific heat and energy all agree with those of Shih and Stroud for similar system sizes. Our largest system size for the honeycomb lattice is 8192, much

larger than the largest system size of 576 studied by Shih and Stroud. As pointed out in section 3.3, on the basis of the saturation of the specific heat with the system size, Shih and Stroud interpreted the transition as being of the KT type. Furthermore, from a study of the helicity modulus they obtained a $T_c$ of 0.12. It is interesting to note that our study of the linear and spin glass susceptibility, in addition to the quantities studied by Shih and Stroud, reveals that the transition is of the spin/gauge glass type, occurring at nearly the same temperature (0.11).

Our results for the quasiperiodic lattices are consistent with those of Halsey [35], who finds a spin glass phase for the frustrated $XY$ model on a square lattice with an irrational flux through the plaquettes. Note that for the Penrose, octagonal, and bathroom tile lattices we can fully frustrate only one of the two elementary plaquettes at any one time, the corresponding flux through the other plaquette being irrational. However, with the example of the honeycomb lattice we have shown that the irrationality of the flux through the plaquettes is not a necessary condition for the existence of the spin/gauge glass phase. It may, however, be a sufficient condition. The common feature of all of the cases studied is that the lattice structure and the transverse magnetic field induce a large number of possible values of the effective coupling parameters $J\cos(A_{ij})$.

The experimental implication of our study is that an array of Josephson junctions, forming any of the lattice structures discussed in this work, in a suitably chosen transverse magnetic field should behave as a superconducting glass at low temperatures. Advanced microfabrication techniques [36] should be capable of generating such periodic/quasiperiodic arrays of superconducting grains. Experimental work of this kind has been reported [37] on 2D fractal (Sierpinski gasket) networks. Halsey [35] has pointed out that for superconducting arrays with low normal-state resistivities the glass transition should basically appear as a mean-field transition, with fluctuation effects being barely observable. For arrays with high normal-state resistivities the fluctuation effects will cause the glass transition to deviate substantially from a mean-field transition, with noticeable system-dependent details. As discussed by Ebner and Stroud [38], an important property of such glassy superconductors is a large difference between their dc and ac susceptibilities.

## Acknowledgments

Financial support for this work was provided by the Natural Sciences and Engineering Research Council of Canada. The authors are grateful to Professor T Soma for providing them with the program for generating octagonal lattices, and to Professor M J P Gingras for useful discussions. Useful comments on our results from Professor A P Young and S Teitel are also gratefully acknowledged.

## References

[1] Reid R W, Bose S K and Mitrović B 1996 *Phys. Rev.* B **54** R740
[2] Strandburg K J 1991 *Comput. Phys.* **5** 520
[3] Chowdhury D 1986 *Spin Glasses and Other Frustrated Systems* (Singapore: World Scientific)
[4] Fradkin E, Huberman B A and Shenker S H 1978 *Phys. Rev.* B **18** 4789
[5] Soma T, Watanabe Y and Ito M 1989 *Proc. 3rd Int. Mtg on Quasicrystals* (Singapore: World Scientific) p 231
Watanabe Y, Soma T, Ito M and Betsumiya T 1987 *Mater. Sci. Forum* **22–24** 213
Niizeki K 1989 *J. Phys. A: Math. Gen.* **22** 1859
[6] Bhatt R N and Young A P 1988 *Phys. Rev.* B **37** 5606
[7] Jain S and Young A P 1986 *J. Phys. C: Solid State Phys.* **19** 3913

[8] Binder K and Young A P 1986 *Rev. Mod. Phys.* **58** 801
[9] Morgenstern I and Binder K 1980 *Phys. Rev.* B **22** 288
[10] Schwartz M and Young A P 1991 *Europhys. Lett.* **15** 208 and the references therein
[11] Lemke N and Campbell I A 1996 *Phys. Rev. Lett.* **76** 4616
[12] Teitel S and Jayaprakash C 1983 *Phys. Rev.* B **27** 598
[13] Shih W Y and Stroud D 1984 *Phys. Rev.* B **30** 6774
[14] Miyashita S and Shiba H 1984 *J. Phys. Soc. Japan* **53** 1145
[15] Lee D H, Caflisch R G, Joannopoulos J D and Wu F Y 1984 *Phys. Rev.* B **29** 2680
[16] Yosefin M and Domany E 1985 *Phys. Rev.* B **32** 1778
[17] Choi M Y and Doniach S 1985 *Phys. Rev.* B **31** 4516
[18] Lee D H, Joannopoulos J D, Negele J W and Landau D P 1986 *Phys. Rev.* B **33** 450
[19] Berge B, Diep H T, Ghazali A and Lallemand P 1986 *Phys. Rev.* B **34** 3177
[20] Lee J, Kosterlitz J M and Granato E 1991 *Phys. Rev.* B **43** 11 531
[21] Granato E, Kosterlitz J M, Lee J and Nightingale M P 1991 *Phys. Rev. Lett.* **66** 1090
[22] Granato E and Nightingale M P 1993 *Phys. Rev.* B **48** 7438
[23] Lee J-R 1994 *Phys. Rev.* B **49** 3317
[24] Ramirez-Santiago G and José J V 1994 *Phys. Rev.* B **49** 9567
[25] Nightingale M P, Granato E and Kosterlitz J M 1995 *Phys. Rev.* B **52** 7402
[26] Kosterlitz J M and Thouless D J 1973 *J. Phys. C: Solid State Phys.* **6** 1181
[27] Kosterlitz J M 1974 *J. Phys. C: Solid State Phys.* **7** 1046
[28] Tobochnik J. and Chester G V 1979 *Phys. Rev.* B **20** 3761
[29] Lançon F and Billard L 1986 *Europhys. Lett.* **2** 625
[30] Reger J D, Tokuyasu T A, Young A P and Fisher M P A 1991 *Phys. Rev.* B **44** 7147
[31] Metropolis N C, Rosenbluth A W, Rosenbluth M N and Teller E 1953 *J. Chem. Phys.* **21** 1087
[32] Edwards S F and Anderson P W 1975 *J. Phys. F: Met. Phys.* **5** 965
[33] Binder K 1981 *Z. Phys.* B **43** 119
Binder K 1981 *Phys. Rev. Lett.* **47** 693
See also
Binder K and Heermann D W 1992 *Monte Carlo Simulation in Statistical Physics (Springer Series in Solid-State Sciences 80)* (Berlin: Springer) section 2.3.4
[34] Toulouse G 1977 *Commun. Phys.* **2** 115
[35] Halsey T C 1985 *Phys. Rev. Lett.* **55** 1018
[36] Prober D E 1984 *Percolation, Localization and Superconductivity (NATO ASI Series B, vol 109)* ed A M Goldman and S A Wolf (New York: Plenum) pp 231–66
[37] Gordon J M, Goldman A M, Maps J, Costello D, Tiberio R and Whitehead B 1986 *Phys. Rev. Lett.* **56** 2280
[38] Ebner C and Stroud D 1985 *Phys. Rev.* B **31** 165